



Imaging in urethral stricture disease: an educational review of current techniques with a focus on MRI

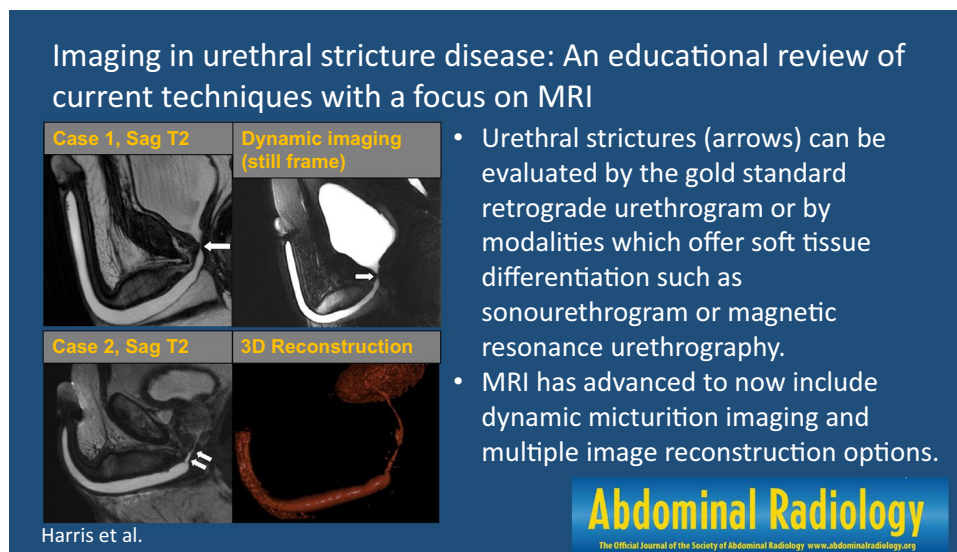
Daniel Harris^{1,3} · Christopher Zhou^{1,3} · Jeffrey Girardot¹ · Ariel Kidron² · Shubham Gupta^{1,2,3} · Andre Guilherme Cavalcanti^{3,4} · Leonardo Kayat Bittencourt^{1,5}

Received: 19 August 2022 / Revised: 28 November 2022 / Accepted: 29 November 2022 / Published online: 28 January 2023
© The Author(s), under exclusive licence to Springer Science+Business Media, LLC, part of Springer Nature 2023

Abstract

Urethral stricture disease refers to narrowing of the urethral lumen obstructing the flow of urine. Urethral strictures can significantly impact daily life due to incontinence, incomplete emptying, hesitancy, and increased risk of urinary tract infections. Imaging is central to the evaluation of suspected urethral stricture, as assessment of stricture length and severity is crucial for guidance of surgical management. The currently employed modalities include radiography, chiefly retrograde urethrography (RUG) and voiding cystourethrography (VCUG); magnetic resonance urethrography (MRU); and sonourethrography (SUG). MRU has become a recent focus of research as it provides high spatial resolution, multiplanar capacity, and soft tissue type differentiation for evaluation of periurethral compartments and concurrent soft tissue defects. The protocol for MRU has evolved over the years to now include dynamic micturition imaging and image reconstruction options. In this review, we discuss each of the imaging modalities used in the diagnosis and evaluation of urethral stricture and provide an overview of literature on MRU over the last decade, including suggested indications that have not yet been incorporated into current guidelines. We delineate scenarios where special diagnostic imaging beyond radiography is beneficial, providing examples from our practice and description of our techniques for each modality.

Graphical abstract



Keywords Urethral stricture · Magnetic resonance urethrography · Diagnostic imaging · Review literature as topic

Extended author information available on the last page of the article

Introduction

Urethral stricture refers to narrowing of the anterior urethral lumen which obstructs the flow of urine [1]. Posterior urethral narrowing is referred to as urethral stenosis. Urethral strictures have a significant impact on daily life with a 41% rate of urinary tract infections (UTIs) and 11% rate of incontinence [2]. Other uncomfortable symptoms can arise from the narrowed urethra causing incomplete emptying, hesitancy, and decreased urinary stream [3]. Interest in optimizing imaging techniques to support the growing capabilities of surgical corrections has grown especially over the last two decades. In this article, we summarize the major developments in imaging of urethral strictures with a focus on the applications of MRI.

The decision to image follows a thorough history inquiring about signs and symptoms (decreased urinary stream, hesitancy, intermittency, dysuria, recurrent UTIs, genitourinary pain, etc.) in the context of pertinent history such as prior pelvic trauma, surgeries, instrumentation, radiation, or injections. Physical exam findings may include palpable bladder, urethral fibrosis or masses, perineal fistulas, or signs of infection. Once a clinical suspicion of urethral stricture arises, both AUA and EAU guidelines recommend ordering non-invasive studies, especially urine flow rate or ultrasound post-void residual assessment. Upon confirming suspicion, clinicians can utilize urethro-cystoscopy, retrograde urethrography (RUG), voiding cystourethrography (VCUG), or ultrasound urethrography to make a diagnosis. Although currently the AUA has no guidance on the usage of magnetic resonance urethrography (MRU), the EAU suggests using sonourethrography (SUG), MRU, and/or antegrade cystourethrography to assess the degree of spongiofibrosis and exact stricture length for guidance of surgical approach. MRU is specifically recommended as an ancillary test for posterior urethral stenosis by the EAU [4, 5].

Recently, a compilation of research has suggested uses of MRU beyond those outlined by the EAU. For the purposes of the practicing urologist and radiologist we have attempted to compile the findings from the case series and give examples from our own institution to summarize. We delineate scenarios where special diagnostic imaging beyond X-ray is beneficial and describe our techniques for each imaging modality.

Definitions, clinical assessment, and treatment modalities for urethral strictures

A urethral stricture arises from the body's response to damaged urethral mucosa and erectile spongy tissue.

Deposition of collagen, referred to as spongiofibrosis when involving the corpus spongiosum, in the affected urethral segment leads to contraction of the urethral lumen. Urethral strictures can occur secondary to numerous pathologies and can affect the entire length of the urethra. Male urethral strictures are the focus of most research, as the prevalence is 229–627 per 100,000 in males while urethral strictures in females are extremely rare [2]. The primary etiology of strictures in resource-abundant countries is idiopathic. Iatrogenic injuries, sexually induced trauma, and urinary catheter-related trauma are also major etiologies, accounting for 45% of strictures cases [6]. Other etiologies include infections, hypospadias repair, inflammatory skin conditions, radiation therapy, other surgical causes, and pelvic traumas such as straddle injuries.

Strictures in the male urethra are classified based on urethral anatomy. Anterior urethra refers to the meatus of penis, fossa navicularis, pendulous urethra, and bulbar urethra, while the posterior urethra refers to the membranous urethra, prostatic urethra, and bladder neck. The urogenital diaphragm of the male urethra demarcates the transition of anterior to posterior urethra (see Example 1 in MRU section for visual anatomy). Due to the lack of corpus spongiosum in the posterior urethra, urethral narrowing in this region is most accurately referred to as urethral stenosis or bladder neck contracture rather than urethral stricture [8]. Outside the urethra, strictures can be associated with soft tissue abnormalities including fistulae, cavitation, diverticula, and false passages [9]. Specific etiologies such as traumatic bulbar strictures are more associated with soft tissue pathologies such as fistulas and diverticula [6].

Strictures are also a frequent complication in transgender patients who have undergone phalloplasty as part of female-to-male gender affirmation surgery [7]. Phalloplasty is a surgical procedure that aims to create a penis-like structure in the perineum for trans men, with goals including some or all of esthetic satisfaction, tactile and erogenous sensation, standing micturition, and the ability to have an erection and penetrative intercourse. Various single- and multi-staged techniques have been described, with commonly used donor sites including the anterolateral thigh (ALT) flap, radial forearm free flap (RFFF), abdominal flap, and superficial circumflex iliac artery perforator (SCIP) flap [10]. For patients who desire the ability to urinate from their neophallus, urethral extension can be performed which requires the creation of a urethral lumen inside the newly constructed penile shaft. This is most accomplished using the tube within a tube (TWT) design, which involves two skin paddles from the donor site that are rolled in opposite directions and placed together with an intervening dermal bridge for blood supply. The native urethra is then lengthened using paravaginal mucosal flaps to create the fixed urethra (*pars fixa*), which

Example 1 Normal sagittal T2 of a non-distended (no gel infusion step) urethra, showing the collapsed appearance of the urethra within the spongiosum and surrounding anatomy. Parts of the male urethra (traced by dotted line and divided by solid white lines):

1. Intramural/preprostatic part originating as continuation of bladder neck
2. Prostatic part (location of seminal colliculus, not visualized)
3. Membranous/intermediate, a naturally narrow portion of the urethra due to passing through the pelvic floor and being surrounded by the external urethral sphincter
4. Bulbous/penile urethra which originates beyond the urogenital diaphragm and passes into the corpus spongiosum of the penis
5. Pendulous urethra which begins at the end of the fan-like suspensory ligament of the penis and dilates in the fossa navicularis before terminating in the urethral meatus

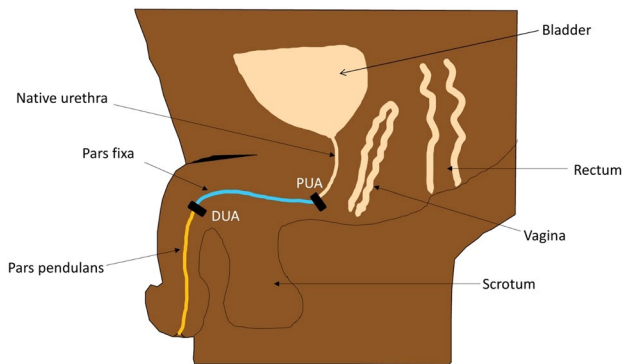
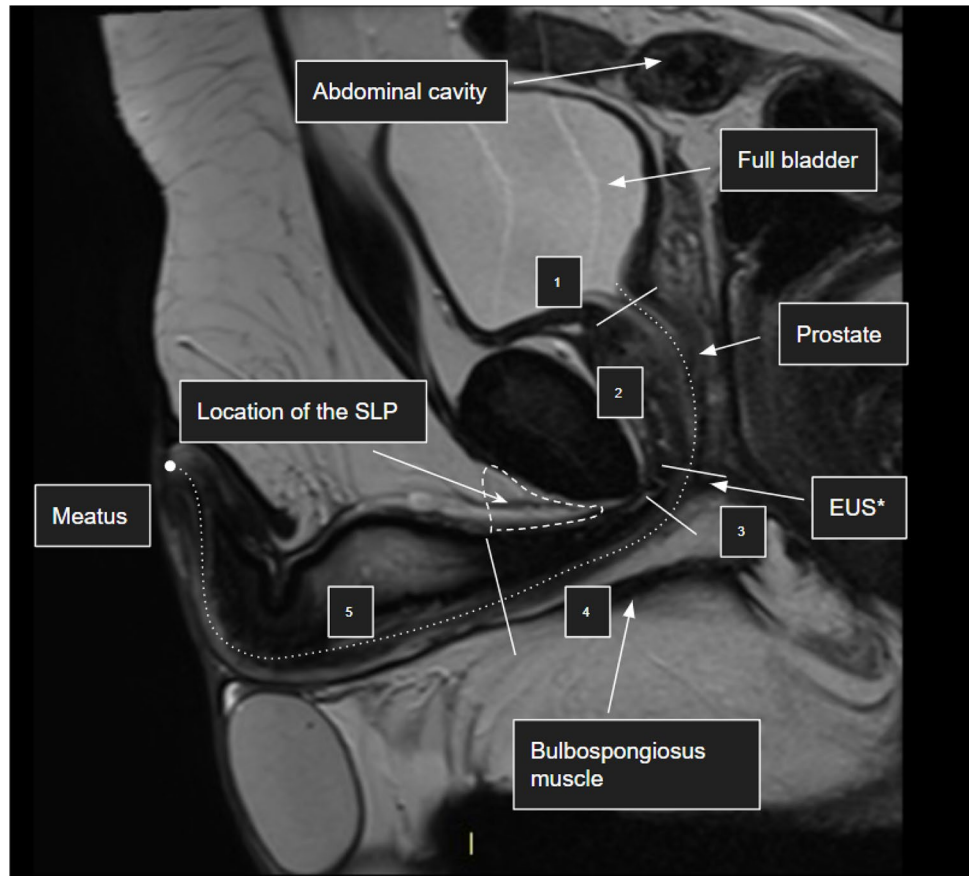


Fig. 1 Anatomy of phalloplasty for patients undergoing female-to-male gender affirming surgery. *PUA* proximal urethral anastomosis. *DUA* distal urethral anastomosis

is connected to the new penile urethra (pars pendulans) (Fig. 1). Strictures are prone to develop at the junction of the pars fixa and pars pendulans due to the use of long, delicate flaps that are anastomosed to the native anatomy [7].

Current treatment options for urethral stricture can be broadly divided into endoscopic and open reconstructive approaches. Endoscopic therapies are further subdivided into dilation techniques and urethrotomy techniques. Direct visualization internal urethrotomy (DVIU) is the standard

endoscopic modality and involves making a camera-guided longitudinal incision along the stricture into healthy, non-scarred urethral tissue. The open edges of the wound subsequently re-epithelialize. Dilation is traditionally performed with a wire-guided balloon or serial plastic dilators. More recently, the paclitaxel-coated Optilume balloon was recently approved by the FDA in 2021 for the treatment of urethral stricture and has demonstrated both safety and superior efficacy out to 6 months compared to other endoscopic options [11]. Surgical reconstruction of the urethra (urethroplasty) is the gold standard of urethral stricture treatment, can be offered as initial therapy for any stricture, and is associated with higher success rates than dilation or endoscopic treatment [4]. End-to-end urethroplasty has the best long-term success of all reconstructive options and involves excision of the diseased urethral segment, followed by anastomosis of healthy surrounding urethral tissue to replace the excised segment (Fig. 2). Free graft urethroplasty typically with a buccal mucosal graft is used for strictures where end-to-end urethroplasty is not possible [3]. Strictures in transgender patients post-phalloplasty are typically managed with anastomotic urethroplasty, with perineal urethrostomy as a measure of last resort after multiple failed attempts [7]. Importantly, spongiofibrosis must be removed during surgical correction of strictures [9]. Imaging is key to selecting a treatment

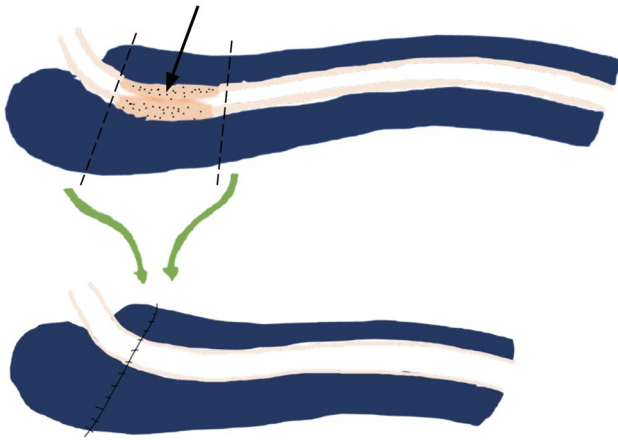


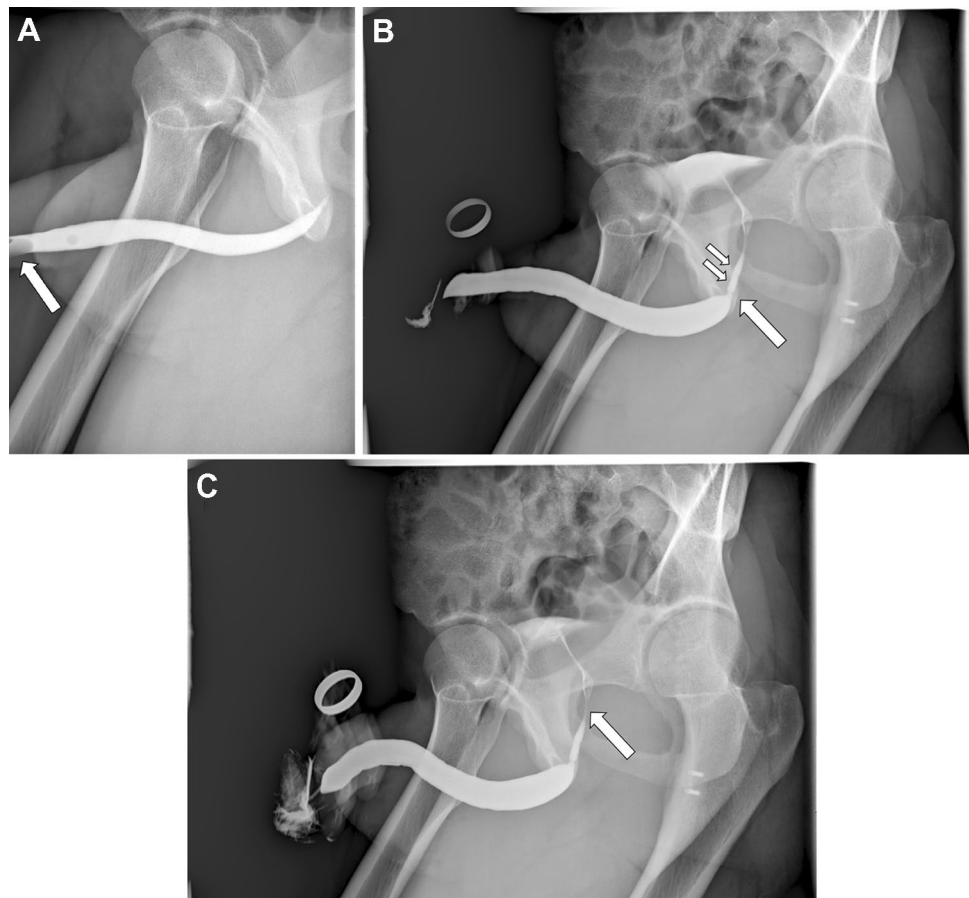
Fig. 2 Example of end-to-end anastomotic urethroplasty. Stricture (black arrow) and associated spongiositis is resected with subsequent approximation of proximal and distal ends (dashed lines) at anastomosis (suture line)

option, and treatment planning can commence once the length, location, and severity of the stricture and the health of surrounding tissues have been ascertained.

Radiography: Retrograde urethrography (RUG) and voiding cystourethrography (VCUG)

Urethral radiography, introduced over a century ago [12], still stands as the most common imaging modality for evaluation of urethral strictures [13]. A 2D radiograph provides information on the number of strictures, stricture length, stricture location, and the caliber of the narrowed lumen, sufficient for describing simple strictures (Fig. 5). Its applications can be extended to transgender patients with stricture post-phalloplasty, where a retrograde urethrogram (RUG) is required at time of surgery to rule out multifocal stricture (Fig. 3) [7]. RUGs benefit from low cost, high availability, a strong body of literature, and years of physician experience. Urologists are extremely familiar with RUGs and identify the presence and length of strictures more accurately in their own patients when compared to independent readers (radiologists) [14]. Radiopaque contrast material injected through the urethral meatus expands the urethra and enhances the lumen. Strictures are visualized as longitudinal or annular narrowing of the urethra (Fig. 3b). When studying strictures, the prostatic urethra and ovoid filling defect created by the

Fig. 3 20-year-old smoker with a history of dysuria and hematuria. Patient later underwent flexible cystoscopy measuring 4.5 cm stricture. **a** Catheter visualized in place with contrast filling to distal end of proximal bulbar stricture. **b** Proximal bulbar stricture and/or membranous stenosis visualized in early voiding phase (catheter removed). Large arrow pointing towards annular stricture. Small arrows point to continued distal stenosis through membranous urethra. **c** Voiding phase demonstrating minimal opening of prostatic urethra (arrow)



verumontanum should not be confused with pathologic stricture (Fig. 3c). A slight indentation of the anterior wall of the proximal bulbar urethra is another confounding finding that resembles an annular stricture but is caused by spasm of the constrictor nudae muscle in reaction to the pushing of contrast.

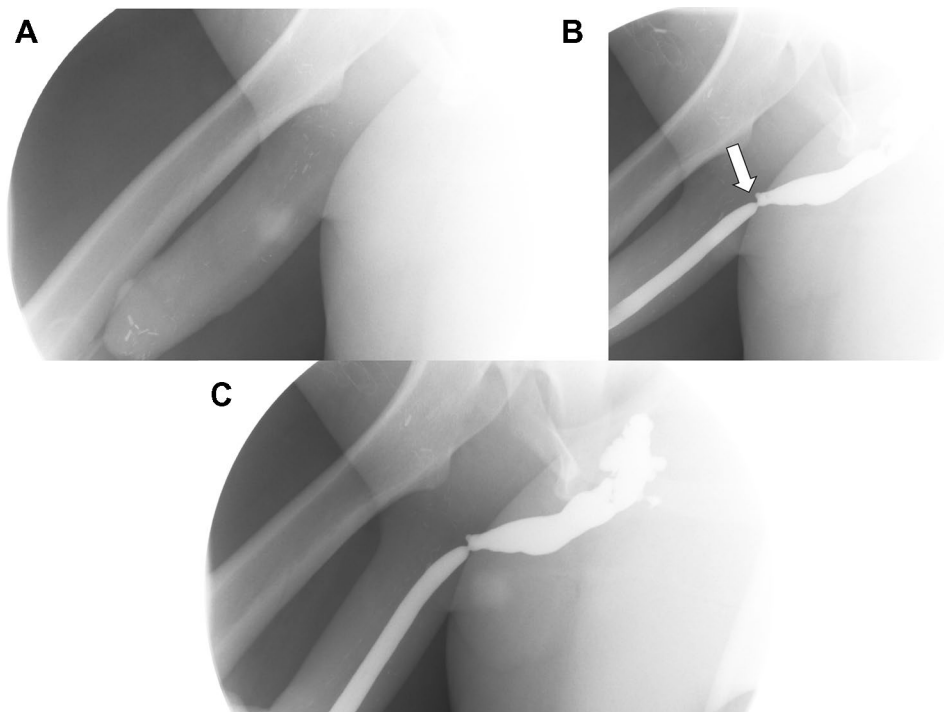
If a RUG provides insufficient distension of the urethra proximal to the stricture, voiding cystourethrography (VCUG) can be utilized immediately during the same study to approach the stricture from the opposite side (Figs. 3c, 4c). VCUG supplements the static films of RUG with dynamic voiding images. The act of micturition distends the bladder neck and posterior urethra. This allows the precise identification of a stricture's proximal point of narrowing, a useful tool when studying obliterative or near-obliterative strictures that are incompletely characterized by RUG. VCUG also provides information on functional impairment caused by the stricture by allowing visualization of urethral distension when voiding [13]. Although time-consuming, the study is highly useful in presurgical planning, especially for patients with multiple strictures.

RUG and VCUG can provide basic stricture morphology even in complex cases, but they lack the ability to show adjacent periurethral soft tissues for surgical planning (Fig. 6). Some soft tissue pathology can be inferred if it alters the path of contrast. For example, fistulas can be seen as extravasation of contrast [15] but still are usually poorly defined [16]. VCUG and/or RUG is often combined with physical exam and cystourethroscopy for surgical planning regarding fistulas. Any other defects that can

appear as simple filling defects can also be visualized on RUG including cavitation or dilatation [17]. These findings can aid in the assessment of the severity of stricture disease such as when a massive dilatation is visualized distal to a stricture indicating severe obstruction.

Practically, RUG is significantly impacted by patient positioning, reflex contraction of pelvic muscles, and adequate maintenance of penile traction [18]. These factors can lead to over and underestimation of stricture length measurements requiring further invasive testing such as flexible cystoscopy or lengthened intraoperative planning. For example, spongiofibrosis encountered during urethroplasty not seen on RUG may cause proximal and distal ends of anastomotic urethroplasty to be longer than expected. Multiple studies comparing RUG to MRU and SUG have found RUG to differ by 0.51–0.70 cm on average to intraoperative stricture measurements, especially at the bulbar site [9, 19, 20]. Measurements created in the image viewing browser (PACS) are approximations corrected for obliquity of the penis and magnification which can contribute to some error. The precision of measurements could impact surgical decision-making especially when the stricture is on the border between a short (<2 cm) and long (≥ 2 cm) strictures. Penile urethral strictures are treated with urethroplasty regardless of length, but treatment of bulbar strictures depends on length. A short bulbar urethral stricture may be treated with a urethral dilation, direct visual internal urethrotomy (DVIU), or a urethroplasty while a long bulbar urethral stricture would best be initially treated with urethroplasty only [3, 4].

Fig. 4 21-year-old transgender male 3 months status post neophallus (radial forearm phalloplasty) with inflatable penile implant followed removal and reimplantation of penile prosthesis due to infection and inflammatory reaction. Later presenting with urinary symptoms. Cystoscopy found pars fixa to be tight with normal appearance of native urethral meatus and rest of posterior urethra. **a** Scout image. **b** RUG shows stricture (arrow) at pars fixa of pendulous urethra and pars fixa. Later cystoscopy found pars fixa to be tight with normal native urethral meatus and urethra. **c** Voiding phase demonstrating dilation proximal to short pars fixa stricture



Standard imaging protocol for RUGs, including the one performed at our institution, is as follows: After micturition, a supine PA scout image is taken with bladder and urethral regions in view. The patient is then laid obliquely (35–45 degrees) and with the dependent leg flexed. Scout images are taken to make sure there was adequate obliquing of the obturator fossa with adjustment as necessary (Fig. 6a). After retracting the foreskin if present, the penis can be gripped with a gauze pad and stretched over the dependent thigh. An 8 French foley catheter is placed per meatus and the balloon is partially inflated in the fossa navicularis, usually requiring 1–2 mL saline to prevent leakage. Unfortunately, lubrication may not allow adequate friction for the balloon and is not recommended. A catheter tip syringe is used to inject 10% water soluble contrast (urographin) in sterile saline requiring 20–60 mL of solution to adequately distend the urethra. Slow, continuous pressure will overcome possible spasm of the external urethral sphincter. Intermittent scout as well as cine images are taken including injection, pre-void, voiding, and post-void images (Fig. 3a–c). Sedation may be necessary in boys and small children to obtain good quality images (Figs. 5, 6).

Sonourethrography (SUG)

Ultrasound urethrography or sonourethrography (SUG) can be used to assess a variety of urethral pathologies, including strictures, diverticula, false passages, fistulas, and calculi [21]. SUG allows for the characterization of exact location, length, and severity of strictures along with the capability of defining periurethral tissues. SUG has been known for decades to clearly show the presence and degree of periurethral spongiofibrosis [22, 23]. Ultrasound has the added benefits of being quick, non-invasive, painless, readily available, and lacking ionizing radiation. The portability of sonography machines allows for usage in most clinical settings, including intraoperatively [24], and without the need for heavy radiologic hardware.

Several studies have shown that ultrasound is as effective at assessing the length and severity of strictures as RUG [25–27]. Ultrasound may be superior to contrast urethrography in visualizing short strictures [28, 29] located within the bulbar urethra [30, 31]. As a soft tissue characterizing imaging modality, SUG allows for characterization of mucosal abnormalities that only appear as subtle filling defects on RUG. Furthermore, SUG enables the visualization of adjacent spongiofibrosis, which is not possible with radiography. The addition of sonoelastography allows qualitative and quantitative measurement of tissue elasticity, a useful marker of spongiofibrosis severity that is correlated with stricture recurrence rate and the difficulty of incising the affected urethral segments. Combined with SUG, sonoelastography

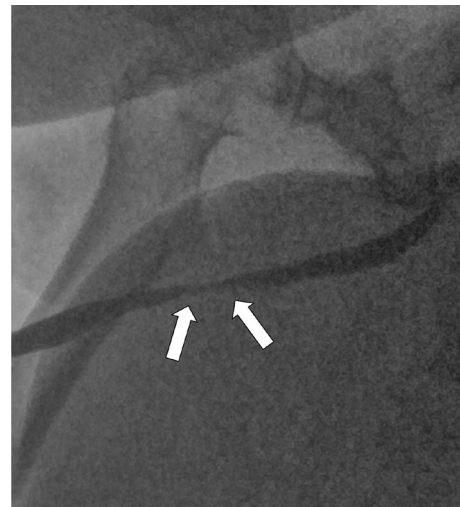
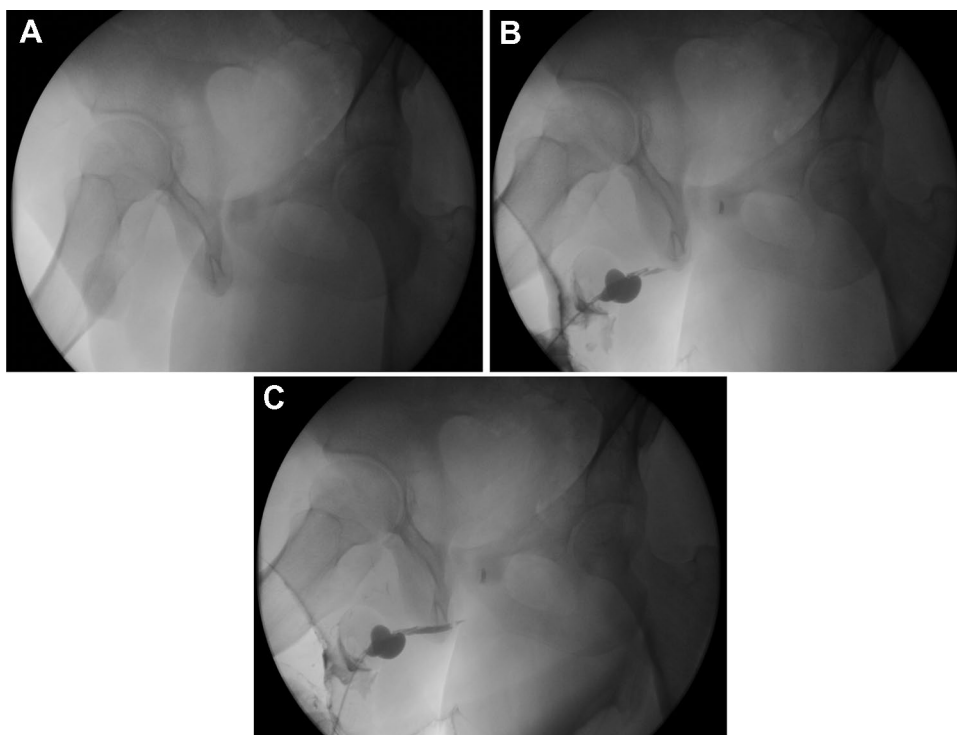


Fig. 5 48-year-old smoker with a history of multiple years of poor urine stream, multiple UTIs, hematuria, multiple kidney stone episodes, and dysuria. RUG showed approximately 2 cm mid-anterior urethral narrowing (arrows) with no evidence of leakage suggestive of bulbar urethral stricture

provides a more accurate estimation of stricture evaluation parameters than RUG [32, 33]. Therefore, SUG has found a role as an adjunctive imaging modality to help guide treatment in patients with known bulbous urethral strictures. In addition to short strictures and anterior strictures, SUG is especially practical in patients who have or are likely to undergo hypospadias repair as hypospadias is commonly associated with strictures [34]. It is however a reasonable acknowledgment that ultrasound evaluation in the pediatric population may be challenging due to a lack of cooperation. Sedation or general anesthesia may be required in babies or small children.

When used to visualize the anterior urethra, SUG can measure strictures to 100% accuracy of actual intraoperative findings, with a reported sensitivity of 86.63% and specificity of 94.66% [35]. Anterior stricture findings evaluated by SUG are comparable to those of MRU [36] and have been demonstrated to impact surgical management in meaningful ways, at times changing the original surgical approach entirely [37]. However, the posterior urethra can only be visualized with 60% accuracy when correlated with intraoperative findings [38], with SUG frequently overestimating stricture length compared to more accurate measurements obtained through MRU [36]. Despite these limitations, the posterior urethral can be better visualized through usage of a linear endorectal ultrasound probe, which allows both anatomical and functional real-time evaluation of the prostatic and membranous urethra [39, 40]. Another option is to utilize both SUG and RUG which when both used to estimate stricture length and location can reach a high sensitivity, specificity, and overall accuracy equal even to MRI [38].

Fig. 6 15-year-old male with a history of hypospadias located at the penoscrotal junction. Status post multiple repairs most recently a TIP style hypospadias repair, now presenting with straining and spraying. **a** Scout image showing adequate obliquing of the obturator. **b**, **c** Post-surgical changes seen including focal dilation of penile urethra and poor filling of and narrowing of subsequent penile urethra. Suggestive of proximal penile stricture. Extent of fibrosis and relation to adjacent soft tissue compartments is difficult to ascertain



Sonourethrography is cost-effective like RUG, but its availability is limited by operator training requirements. The procedure may require general anesthesia or otherwise present an uncomfortable experience for the patient as the injection period is generally longer than RUG [38]. Like with RUG, the small field of view may also hinder ease of viewing by the surgeon and flexibility to view structures freely. Nevertheless, the ultrasound probe can be moved along the length of the penis to extend the scan to the perineal area.

SUG begins with a Foley catheter inserted into the decontaminated meatus up to the distal segment of the urethra. The catheter's balloon is filled up to a follow of up to 2 mL to stabilize the catheter at the level of fossa navicularis. A penis clamp may also be used as an alternative to the catheter. A peripheral venous catheter can be used instead of a Foley catheter in patients with meatal stenosis, to deliver fluid to the urethra. The most widely used technique for delivering fluid is the delivery of between 20 and 100 mL of 0.9% NaCl solution through the catheter. Gel use is not recommended as it may result in the generation of artifacts during installation and extension of the urethra. The use of aqueous solution rather than gel unfortunately requires the uncomfortable insertion of the catheter and balloon which can be avoided by imaging procedures that utilize gel such as MRU. Immobilization of the penis by surgical tape on the midline of the hypogastric region is recommended to facilitate proper positioning during the procedure. A high-frequency (15–18 MHz) linear probe is placed on the ventral penis for axial and longitudinal views. A 9–12 MHz probe on the

perineal area visualizes bulbar strictures [21]. The dilated urethra appears as a hypoechoic band (8–10 mm in diameter) with urethral strictures appearing as thick, irregular zones varying in echogenicity (Fig. 7). Assessment of the distal penile urethra is done by completing the examination during the voiding phase, which generates stretching of the urethra and thus allows a better examination of potential pathologies within the urethra.

The EAU does not specifically recommend ultrasound assessments of the urethra but proposes its use in the outpatient setting provided sonourethrography specialization training becomes more widespread [41].

Magnetic resonance urethrography (MRU)

MRU provides high spatial resolution, multiplanar capacity, and soft tissue type differentiation. The high soft tissue contrast allows for the evaluation of periurethral compartments and adjacent anatomical complications. In the setting of urethral strictures, MRU offers the ability to study bladder hypertrophy and trabeculae, proximal dilation of the urethra, prostate volume, and periurethral tissue. Examination of periurethral tissue may reveal fistulae, cavitation, diverticula, false passages, or incidental findings such as tumors. Importantly, associated spongiofibrosis length (SFL) can also be quantified [9, 20]. SFL predicts operation time with moderate strength as well as intraoperative blood loss [9]. Knowing the extent of scar tissue, the surgeon may opt

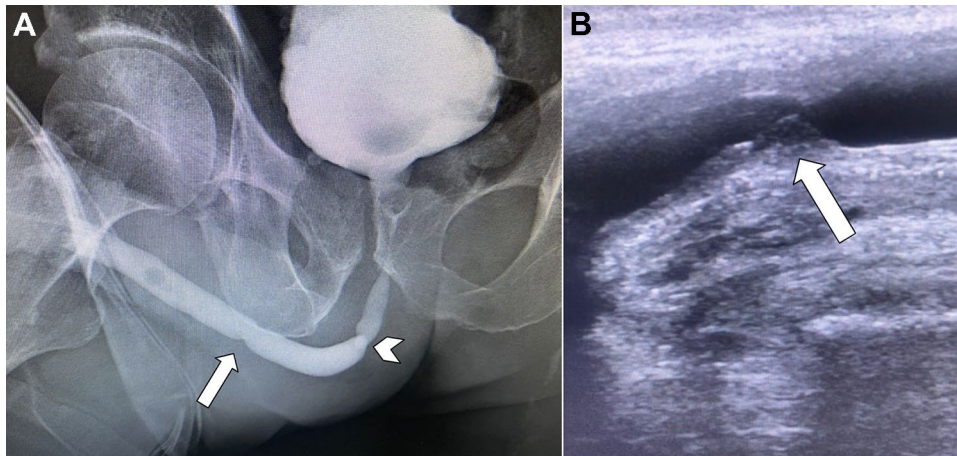


Fig. 7 Multi-modal analysis of stricture using RUG and SUG. **a** RUG demonstrating two areas of narrowing, a mild annular stricture in the penile urethra (arrow) and an annular stenosis in the distal posterior urethra (arrowhead). The annular stenosis still permits retrograde

filling of the bladder. **b** SUG again demonstrates annular stricture in penile urethra (arrow). Hypochoic material contributing to stenosis visualized on SUG in the gel filled urethra. Hypochoic portion of the stenotic segment indicates extent of spongiofibrosis

to utilize steroids to inhibit postoperative regeneration of scar tissue [20]. As mentioned prior, the only current recommended use of MRU is in posterior urethral stenosis to evaluate spongiofibrosis, but literature over the last decades has built up a broad range of uses for MRU not yet captured in AUA or EAU guidelines. We will discuss somewhat chronologically how MRU protocol and technique have evolved and have included the landmark findings from each progressive study in a table (Table 1). Normal anatomy of a non-distended male urethra can be seen in Example 1 for reference.

Dixon first published the usage of regular MRI for study of urethral strictures in surgical planning in 1992 [42]. In 2005, Sung et al. added a gel infusion step which involved dilating the urethra with an injection of 8–10 ml of K-Y jelly into the urethral meatus and tying the glans with long gauze as well as adding post-contrast images [43]. The use of gel infusion and contrast enhancement allowed particularly improved visualization of fibrosis seen as low intensity on T2-weighted (T2W) and post-contrast T1-weighted (T1W) images while surrounding intact corpora spongiosa enhances strongly (Fig. 9). Gel is superior to saline in that it can be injected into the meatus prior to starting MR imaging since it does not leak, and the use of lidocaine gel specifically can ease pain. Overall, the Sung study found MRU to be more accurate to intraoperative findings (MRU error: mean 0.31 cm, median 0.3, range 0–1) than RUG combined with VCUG (RUG error: Mean 1.69 cm, median 1.75, range 0.3–2.8) (Table 1, Column 2). These findings were confirmed by future studies [16, 20, 36, 44, 45]. The next year, Osman et al. utilized a simple MRU protocol of only T2W images with distension of the urethra and reinforced the concept that MRU can reveal extensive

spongiofibrosis extending beyond what appears to be a short stricture on RUG (Table 1, Column 3). Without finding a difference in crude overall diagnosis of confirmed *short* strictures, Osman et al. suggested MR urethrography may be best restricted to extensive strictures to reduce cost and maximize benefit to the patient [16]. However, what is a short stricture with extensive spongiofibrosis will only be revealed by imaging with soft tissue capabilities.

Oh et al. continued forward the usage of T2W in combination with contrast-enhanced T1W images in trauma-associated strictures, emphasizing its ability to delineate proximal urethral morphology in cases where intra-urethral saline or jelly cannot pass through the tight stricture [44] (Table 1, Column 4). In the post-traumatic setting, MRU also provides accurate measurements of extensive strictures, scar tissue, and prostatic displacement. Post-traumatic patients may have diminished bladder capacity after suprapubic diversion of urine and may not tolerate bladder distention to open the bladder neck. In these cases, MRI can provide information without distention although limited. Moving forward to 2019, Tao et al. expanded the MRU protocol to include more viewing dimensions in the T1W post-contrast images (sag, axi, cor) which were now shown to strongly delineate healthy versus fibrosed spongiosum [20] (Table 1 Column 5). Figure 10f provides an example of post-contrast T1W spongiofibrosis. In addition to spongiofibrosis, Tao et al. detailed how edema appears on MRU and suggested that measurement of fibrosis and edema could be used as a quantitative tool to evaluate therapeutic effect of surgery (Table 1 Column 5). Tao et al. first described a voiding technique, analogous to VCUG, in which the patient is instructed to urinate to visualize the proximal urethra [20]. Figure 10 shows utilization of

Table 1 Application of MRI and MRU in case series

Author, year	Sung et al. 2006	Osman 2006	Oh 2010	Tao et al. 2019
No. patients	12	20	25	87
Application	Trauma-associated strictures (straddle, iatrogenic, pelvic fracture) [9], post-radical prostatectomy stricture [1]	Post-inflammatory, iatrogenic [16], post-traumatic [2], posttraumatic [2]	Trauma-associated strictures [24], post-radical prostatectomy stricture [1]	Anterior strictures due to trauma (straddle injury, iatrogenic) and inflammation; posterior strictures due to pelvic trauma and iatrogenic
Imaging protocol	1.5 T: T2W (sag, axi), T1W pre/post (sag, axi)	1.5 T: T2W (sag with reprocessed axi, cor, & obl)	1.5 T: T2W (sag, axi), T1W pre/post (sag)	3.0 T: T2W FS (sag, axi, cor), T1W FS pre (axi), T1W FS post (sag, axi, cor)
Key findings	MRU with distension of the urethra using lubricating jelly is more accurate at measuring stricture length Spongiofibrosis is strongly visible as low T1W intensity with use of distension and contrast MRU caused the urologist to change surgical approach in 7 of 10 patients	Between MRU and RUG, crude overall diagnosis was similar when studying short (< 1.5 cm) strictures but RUG can cause false increase in length MRU can show extensive spongiofibrosis around short strictures and other perirethral soft tissue pathology like tumor, small diverticulae, and fistula	Mean measurement error for MRU is significantly lower than that of RUG + VCUG, compared to surgical measurement. (MRU error \pm SD: 0.4 ± 0.4 vs. RUG SD 1.4 ± 1.1 cm). Suggested MRU as the best imaging modality to assess posttraumatic pelvic anatomy Suggested use of MRU to reveal complete/long defects missed by RUG/VCUG as well as depicting the non-distended urethra proximal to the defect	The stricture length measured by conventional X-ray urethrography [2.17 ± 0.65 cm] was much longer than that measured by MR urethrography [1.68 ± 0.67 cm] Edema around urethra manifests as low intensity on T1W, high intensity on T2W, and no contrast enhancement on T1W
Author, year	Horiguchi 2020	Joshi 2021	Frankiewicz et al. 2021	
No. patients	89	40	55	
Application	Traumatic bulbar stricture [89]	PFUI [40]	Iatrogenic anterior and posterior urethral strictures	
Imaging protocol	3T or 1.5T: T2W (sag, axi)	T2W (sag) while attempting void with full bladder	1.5 T: 3D T2W (sag), T2W (axi), volumetric T1W pre and post (sag)	
Key findings	MRU provides description of soft tissue which helps predict traumatic bulbar stricture repair complexity and plan operation Stricture length, spongiofibrosis length, and proximal bulbar length predict operation time Spongiofibrosis length and proximal bulbar urethral length predict blood loss	Provide protocol designed specifically for evaluation of pelvic fracture urethral injuries using lidocaine jelly for patient comfort Pre-medicated with selective alpha blocker to open bladder neck Focuses on evaluation of urethral gap, orientation of posterior urethra, and relation of posterior urethra to rectum but could be used in the description of strictures	Utilized free open-source software to segment urethra and generate 3D virtual models of urethra which color codes pathologic tissue surrounding urethra Utilized 3D printing to create life-size, patient-specific models	

Columns describe studies conducted and impact on imaging protocol from each respective manuscript. Recent trauma within months will cause contrast enhancement

Axi axial, Cor coronal, FS fat-suppressed, MRU magnetic resonance urethrography, PFUI pelvic fracture urethral injury, RUG retrograde urethrography, Sag sagittal, T1w T1-weighted, T2w T2-weighted, T tesla, VCUG voiding cystourethrography

dynamic imaging to visualize a bulbar segmental stricture coinciding with a rectovesical fistula.

With the complexity of traumatic strictures and related soft tissue changes, clinicians have pursued MRU to provide more detailed information for planning surgical repair of trauma-related strictures [9, 45–47] (Table 1 Columns 6, 7). The complexity of bulbar stricture repair can be predicted by MRU findings of tunica albuginea continuity, periurethral fistula, spongiofibrosis length, and distal and proximal bulbar urethral length relative to the stricture [9] (Table 1 Column 6). Stricture length (OR 1.24) and disruption of tunica (OR 4.17) independently predict the need for corporal splitting when performing excision with primary anastomosis [9]. Expanding the options for MRU protocol, Joshi provides a “Joshi protocol” which involves pre-medicating with a selective alpha blocker to open the bladder neck and evaluate pelvic fracture urethral injuries [46] (Table 1 Column 7). Although urethral trauma imaging focuses on urethral gap and orientation of the posterior urethra, urethral stricture disease and trauma evaluation are often coinciding and can be evaluated together with MRU. A key point is *MRU should be utilized in stricture cases with complex surrounding soft tissue changes* which may be trauma or may be post-surgical changes (Fig. 8) or radiation therapy (Fig. 11). Another recent step forward in MRU is free open-source software that can generate 3D models of the urethra with color coding of pathologic tissue or create life-size patient-specific models for surgeons to study [36] (Table 1 Column 8). Like other reconstructive surgeries, these 3D models may become a core component of surgical planning especially in complex cases. These may be used in combination with reconstructed MRI images as we include in our protocol described below.

Our imaging protocol consists of an axial T1W, T2W axial and sagittal, 3D T2W coronal, MIP sagittal, and T1W

fat-sat sagittal images before and after gadolinium (Fig. 9). Measurements may be made of stricture, surrounding spongiofibrosis, distal bulbar urethral length (distal end of spongiofibrosis to penoscrotal junction) and proximal bulbar urethral length (proximal end of spongiofibrosis to departure of anterior urethra) (Fig. 12). Prior to beginning the procedure, peripheral venous access is obtained and 500 ml of saline is administered intravenously. The operator degerms the field, instills gel, and then nooses the penis with sterile gauze to maintain urethral expansion (See Fig. 13 for detailed instructions). T2w urographic effects images are obtained during rest and micturition strains. The prostatic urethra will open up and images can be captured in 1–2 s intervals (Fig. 10c, d).

At our institute, we have added reconstructed views to our imaging set that may be beneficial to the urologist and radiologist team. Curved planar reformation is a technique used in vascular imaging that can be applied to the curved male urethra (Fig. 9d). This view allows easier viewing of the strictures in a longitudinal fashion. However, this technique should not be interpreted alone as some parts of non-stenosed urethra may appear stenosed. For additional anatomical mapping, 3D reconstruction can be performed (Fig. 11d). This technique provides a high-resolution interactive model for the surgeon to guide surgical approach. Contrast images are taken using gadolinium-based contrast agent (GBCA) at 0.2 mL/kg. This view may allow for easier measurement of spongiofibrosis length.

Despite the strengths of MRU in visualizing both the urethra and surrounding tissues with high resolution, the modality is not without limitations. MRI has many practical limitations (cost, availability) and some functional limitations. We will discuss functional limitations first and discuss the practical separately. The curved planar reformat

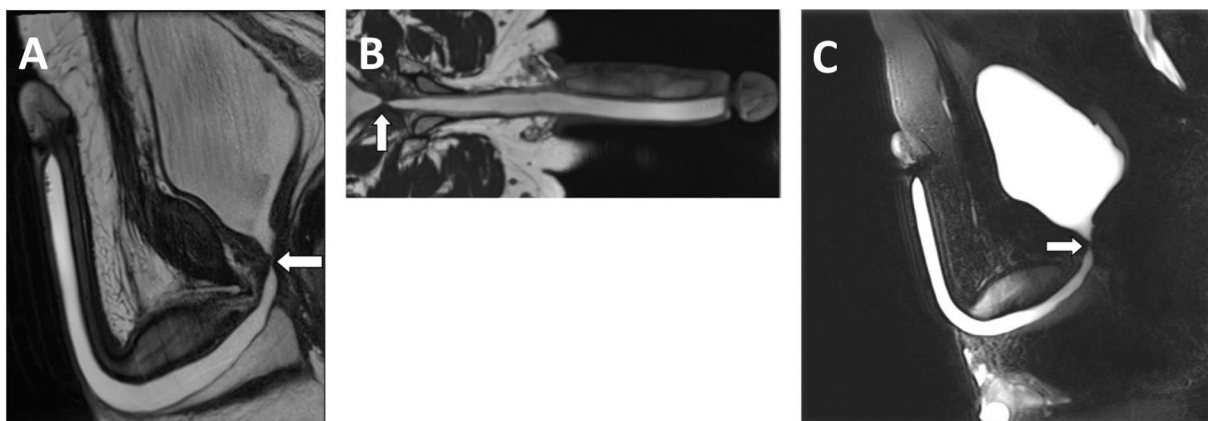


Fig. 8 71-year-old status post-radical prostatectomy with signs of local recurrence. Stenosis visible at site of vesicourethral anastomosis. **a** T2 sagittal image showing near complete loss of continuity between gel-dilated urethra and bladder neck (arrow). **b** Curved reformat

mat showing stenosis and surrounding hypodensity representing post-surgical fibrosis/scar (arrow). **c** Still-frame from MIP sagittal voiding imaging shows failure of stenosis to functionally dilate (arrow)

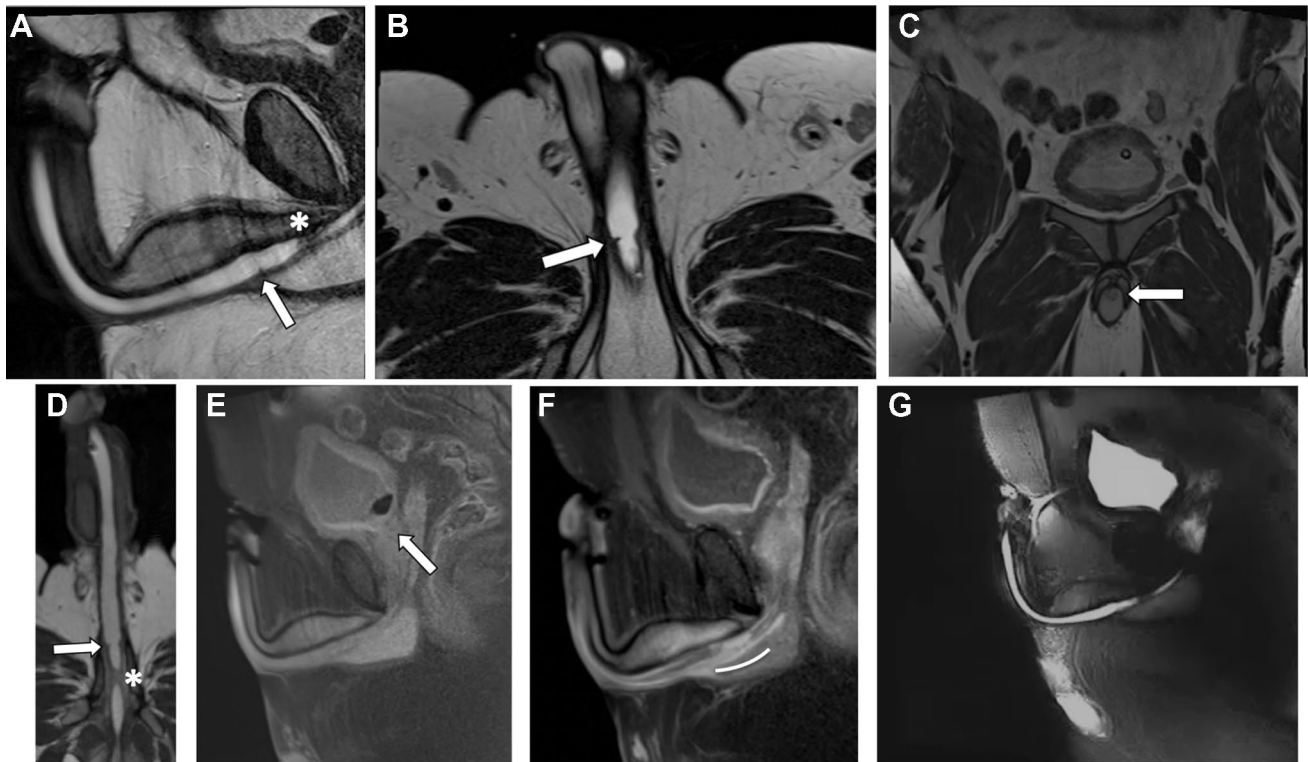


Fig. 9 40-year-old with new onset urinary symptoms after UTI with incidental bladder stone. **a** T2 sagittal: Annular stenosis of distal bulbar urethra seen as circumferential hypointensity surrounding the urethra (arrow). Segmental stenosis of proximal bulbar urethra seen as narrowing of contrast-enhancing urethral lumen surrounded by hypointensity (asterisk). **b** T2 axial: Annular stenosis of distal bulbar urethra (arrow) can be seen in the axial view as circumferential hypointensity surrounding the urethra with expansion of urethra distal to stenosis. **c** 3D T2 coronal: Hypointensity overlying the bulbar urethra (arrow) suggests spongiofibrosis. **d** Curved reformat of T2-Sag: Short annular stricture of distal bulbar urethra (arrow) as well as a segmental stenosis of the proximal bulbar urethra (asterisk). T2 hypointensity underlying the mucosa within the proximo-

stenosis (associated with delayed contrast enhancement) suggests a component of spongiofibrosis. **e** T1 FS sagittal: MRI may reveal unrelated but important pathologies such as this bladder stone (arrow) seen in fat-suppressed T1 sagittal image. **f** T1 sagittal with contrast: T1 post-contrast displays stenosis and underlying spongiofibrosis (white curve) as area of delayed enhancement compared to adjacent healthy corpora spongiosa and thickened walls of the urethra. Diffuse urothelial enhancement of the bladder related to recurrent infection. Hypointensity and associated delayed contrast enhancement of underlying mucosa within proximal stenosis suggests component of spongiofibrosis. **g** MIP sagittal voiding: There is minimal flow of contrast between the bladder and the distal longitudinal bulbar urethra stenosis

technique is known to generate false positive stenoses if the reconstruction plane is not accurately aligned with the course of the urethra [47]. However, since the publication of this data in 1998, software has improved and as described above, the overall accuracy and precision of MRI is still much higher than X-ray. During MRU, the patient is asked to strain (increase intraabdominal pressure) to open their bladder neck. This straining may be difficult for the patient or may not be adequate which can seriously limit readability especially in the case of posterior stenosis. Although MRI provides higher diagnostic capabilities, studies often report unchanged success rates of surgeries [9]. However, this does not consider how outcomes would change if a different surgery was chosen based on the imaging modality, only that the chosen surgery was successful. If the higher accuracy of MRU would change the surgical approach from an excision and end-to-end anastomosis to a urethral dilation and direct

vision internal urethrotomy, the patient's recovery may change. Another consideration when choosing a modality is that many of the recent MRU case studies have taken a focus on the post-traumatic population and may not always be generalizable.

A current well-known downside of any MRI technique is the cost and availability of machinery. Insured males with urethral stricture disease already spend almost 3 times more on healthcare than insured males without stricture disease [2] and an MRI bill adds further to this burden to the patient and society. However, this should be balanced with the potential to prevent repeat urethrotomies or surgical complications with more accurate image-based surgical planning. The national average cost of a pelvic MRI in the USA is \$2550 which is expensive compared to average costs of \$525 and \$400 for pelvic ultrasound and

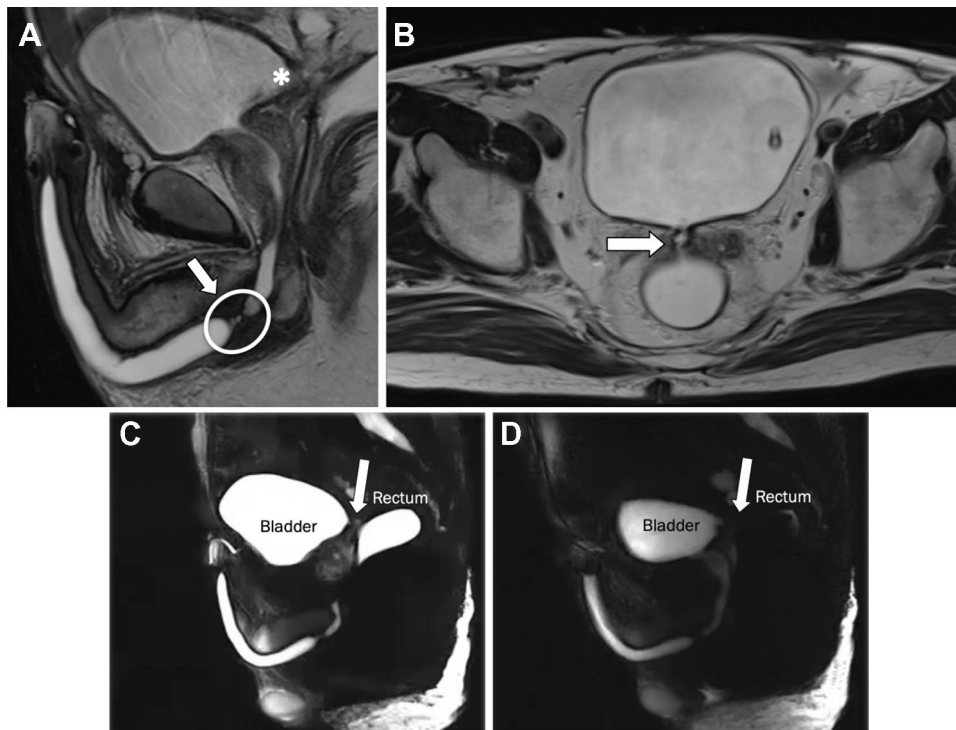


Fig. 10 50-year-old patient status post colorectal surgery complaining of dysuria and fecal incontinence with watery diarrhea. **a** T2 sagittal image showing bladder entrance of rectovesical fistula (asterisk) as irregularity of posterior bladder wall abutting the anterior wall of the rectum next to the side of post-surgical changes. A bulbar segmental stricture with surrounding fibrosis seen as hypointensity surrounding the irregular stenotic section in the bulbar urethra (arrow). **b** T2

axial shows communication between rectum and bladder (arrow) as communicating enhancement with rectum distended with fluid. **c, d** Sagittal T2-FS MIP shows filling of rectum with flow artifacts during voiding and temporary distension of the prostatic and membranous urethra. Rectovesical fistula is visible (arrow). Full dynamic cineclip can be found at <https://tinyurl.com/2vuwyxaw>

X-ray, respectively [48]. Insurance coverage for MRI may also be delayed or not provided especially if the insurance is government. Ultrasound also has limitations in availability of skilled technicians and the presence of a radiologist or urologist trained in this technique, which makes RUG the most accessible imaging. When choosing imaging modalities, the clinician should weigh costs to the required accuracy and soft tissue evaluation for their patient case. Beyond cost, the timely availability of an imaging modality can be critical for surgical planning. Depending on the institute, MRI may only be available on a timeline of days or weeks, and SUG similarly is dependent on sonographer schedule. RUG is a standardized procedure that is typically widely available in a timely manner. Practically, MRU is not standardized in diagnostic workflows for urethral strictures and physicians will need to look to literature to learn appropriate uses. When considering MRI, the provider must also keep in mind general safety concerns of metallic objects, implants and devices (ICDs, cochlear implants, etc.), and dangers of gadolinium (impaired renal function) (Figs. 12, 13).

Example case: Comparison of modalities

We present a 60-year-old male with a history of complete urinary retention secondary to benign prostatic hyperplasia (BPH) status post suprapubic cystostomy. The patient initially underwent holmium laser enucleation of the prostate (HoLEP), an effective transurethral therapy with a reported 3-month catheter-free rate more than 98.5% [49]. During the procedure, cystoscopy showed a normal anterior urethra and bilobar enlargement of the prostate around the posterior urethra. After en bloc technique laser incisions were completed successfully and the prostate enucleated, multiple small adenomas were also removed. Post-operatively, the patient voided successfully but again required the use of his suprapubic cystostomy tube (SPT) to drain a week later. A trial of tamsulosin was unsuccessful. During the second evaluation, cannulation of the suprapubic catheter with flexible cystoscopy found complete obliteration of the bladder neck, a rare and unfortunate complication of transurethral prostate surgery with a reported incidence of 0.3–9.7%. Rates of bladder neck contracture appear to be approximately equal between transurethral resection and

Fig. 11 77-year-old male post-brachytherapy for prostate cancer, now complaining of dysuria. **a** T2 sagittal showing irregular segmental stenosis of the membranous urethra, measuring 2 mm in diameter. **b** Sagittal T1 fat-saturated showing susceptibility artifacts consistent with brachytherapy seeds (arrowheads), with one of them (arrow) apparently crossing through the membranous urethra. **c**, **d** 3D MIP and 3D-rendered reconstructions

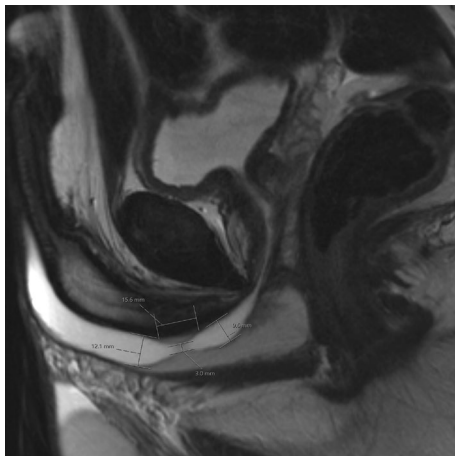
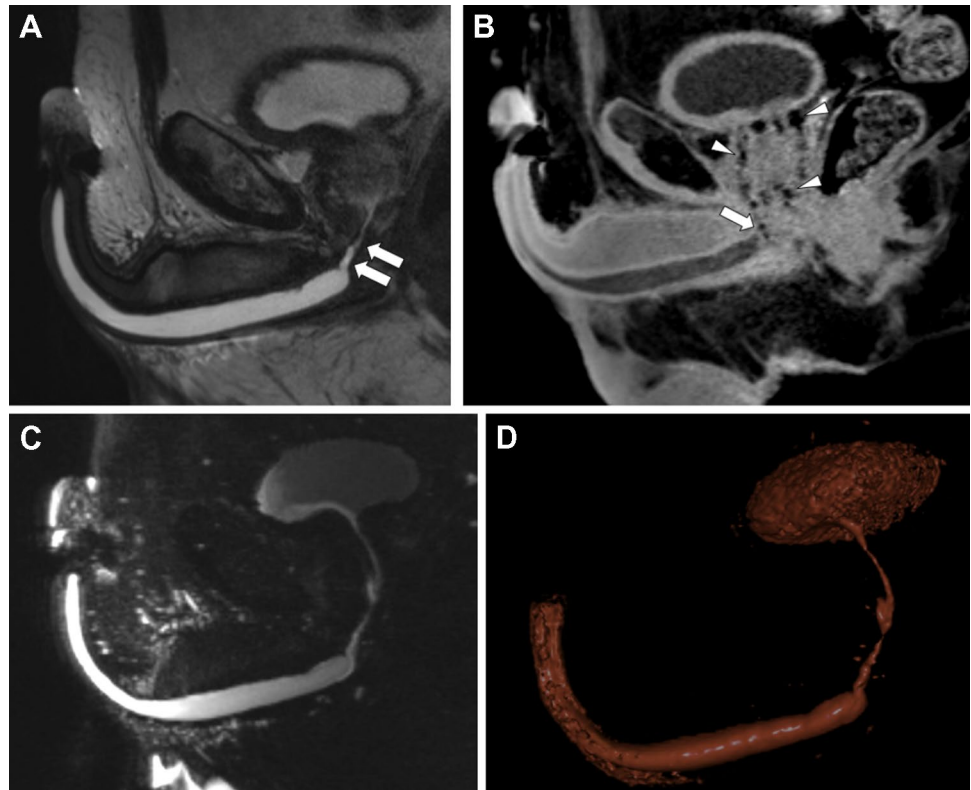


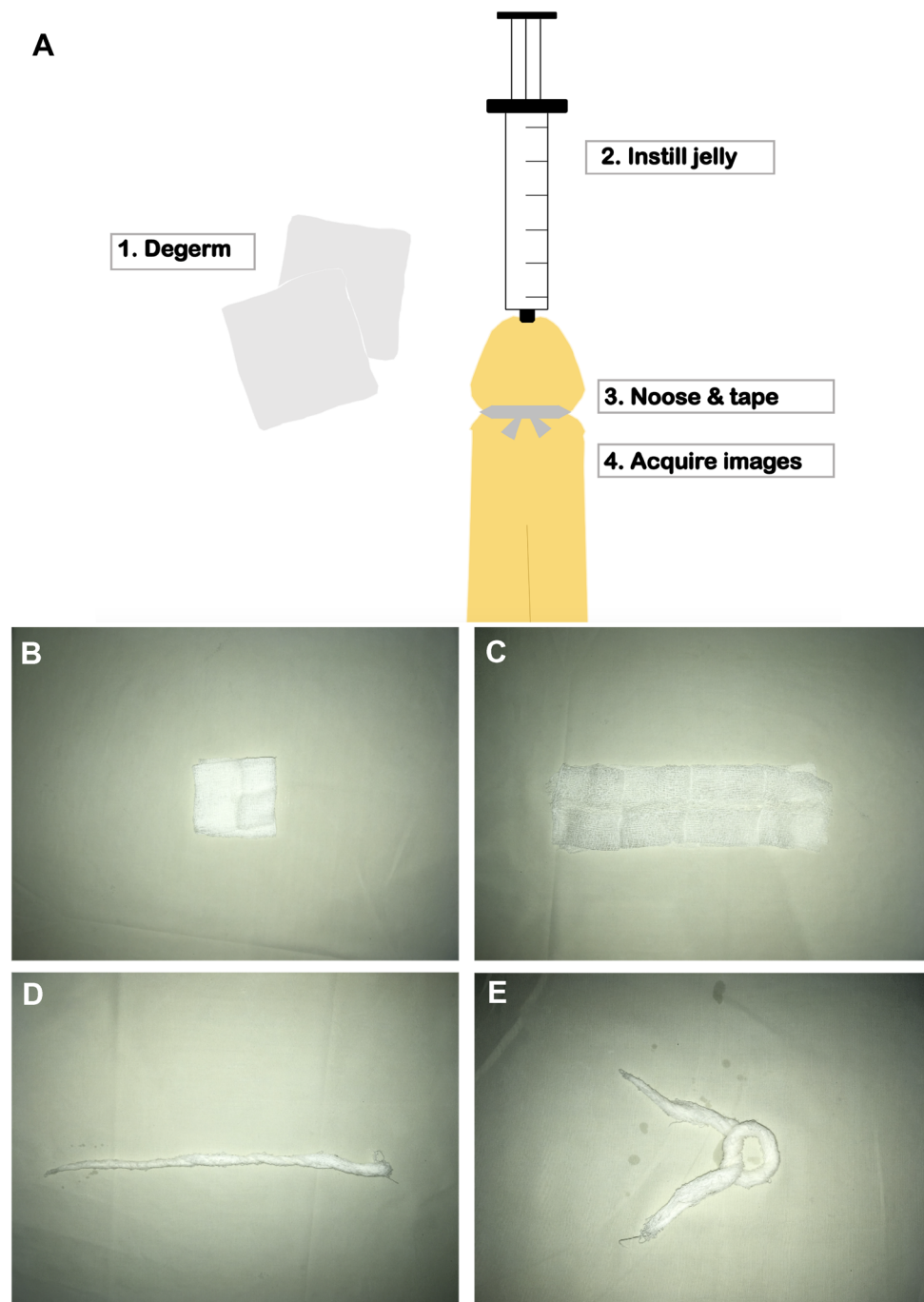
Fig. 12 Longitudinal stricture of the bulbar urethra in a T2W fat-suppressed image. Measurements are made of the urethral diameter proximal and distal to the stricture as well as the length of fibrosis seen as encroaching hypointensity. Fibrosis can be confirmed with post-contrast images showing delayed enhancement

HoLEP [50], and these patients can be effectively treated with a subsequent enucleation procedure [51].

Under continued anesthesia after the cystoscopy, a cystogram and retrograde urethrogram were performed to visualize the extent of stenosis beyond the bladder neck. 300 mL of contrast was instilled through the suprapubic

catheter for a cystogram. Next, a RUG was performed. The intraoperative RUG combined with cystogram showed inability to retrogradely push contrast past bladder neck (Fig. 14a). Although the RUG showed an area of complete stenosis consistent with cystoscopy findings, the patient required further evaluation of the stenosis position and the role of his prostate in the stenosis. The specific capture angle of the intraoperative RUG poorly visualized the anterior to posterior relationship of the posterior urethra and the bladder neck. The multi-department team planned to perform an MRI urethrogram to simultaneously evaluate the prostate and urethral stenosis. The use of MRI in this case provided information on the state of the prostate, the exact length and position of the stricture, fibrosis around the urethra and bladder neck, and an evaluation of the patent membranous urethra for future surgical planning (Fig. 14b–f). Multiplanar MRI of the pelvis was obtained including T2-weighted SSFSE, T2 FSE with and without fat saturation, diffusion-weighted imaging, and pre and post-contrast T1 images. Thanks to the information gleaned from these images, the decision was ultimately made for the patient to undergo robotic simple prostatectomy with urethroplasty and primary anastomosis of the membranous urethra to the bladder neck. The patient regained the ability to void following this surgery, and one year postoperatively he continues to void with a reasonable stream. In this example, an MRU allowed for simultaneous

Fig. 13 MRU protocol at our institution. **a** Step-by-step description of protocol. (1) Degerm glans and penis with chlorhexidine. (2) Instill 10–40 mL of lidocaine hydrochloride jelly 2% (20 mg/mL) through the urethral meatus with 60 mL syringe or a pre-packaged injector. If the tip does not fit to the external walls of the urethra, a urinary catheter can be attached to the syringe tip. While injecting, feeling the spongiosum with a free finger or with the alternate hand allows the operator to know when the spongiosum is turgid indicating fullness. (3) Noose the balanopreputial/retroglandular sulcus with sterile gauze tightly enough to maintain urethral expansion (see **b–e**). The loose ends of the gauze are fixed with tape and the penis is secured to the body with tape. (4) Acquire images. To capture real-time dynamic images during the voiding phase, the patient is instructed to void with the noose still in place, to prevent the need to reposition the patient. **b–e** Steps for creating gauze noose



evaluation of a severe posterior urethral stenosis with a complex history and evaluation of the prostate.

Conclusion

MRI urethrography is a powerful imaging modality that has now been studied for decades as a tool for evaluating urethral stricture disease. MRU provides high accuracy to intraoperative findings, characterizes adjacent soft tissue,

and delineates spongiofibrosis well with the use of T2W and post-contrast T1W images. Dynamic imaging, selective alpha blocker pre-medication (“Joshi protocol”), 3D reconstructions, and open-source software for color-coding tissue are all options for the clinician to plan surgical reconstruction. Still, X-ray urethrography remains the gold standard and most used technique. Its advantages lie in its ability to quickly assess the length, location, and quantity of strictures, low cost, and the benefit to clinicians of over a century’s worth of research and practice. However, it is limited

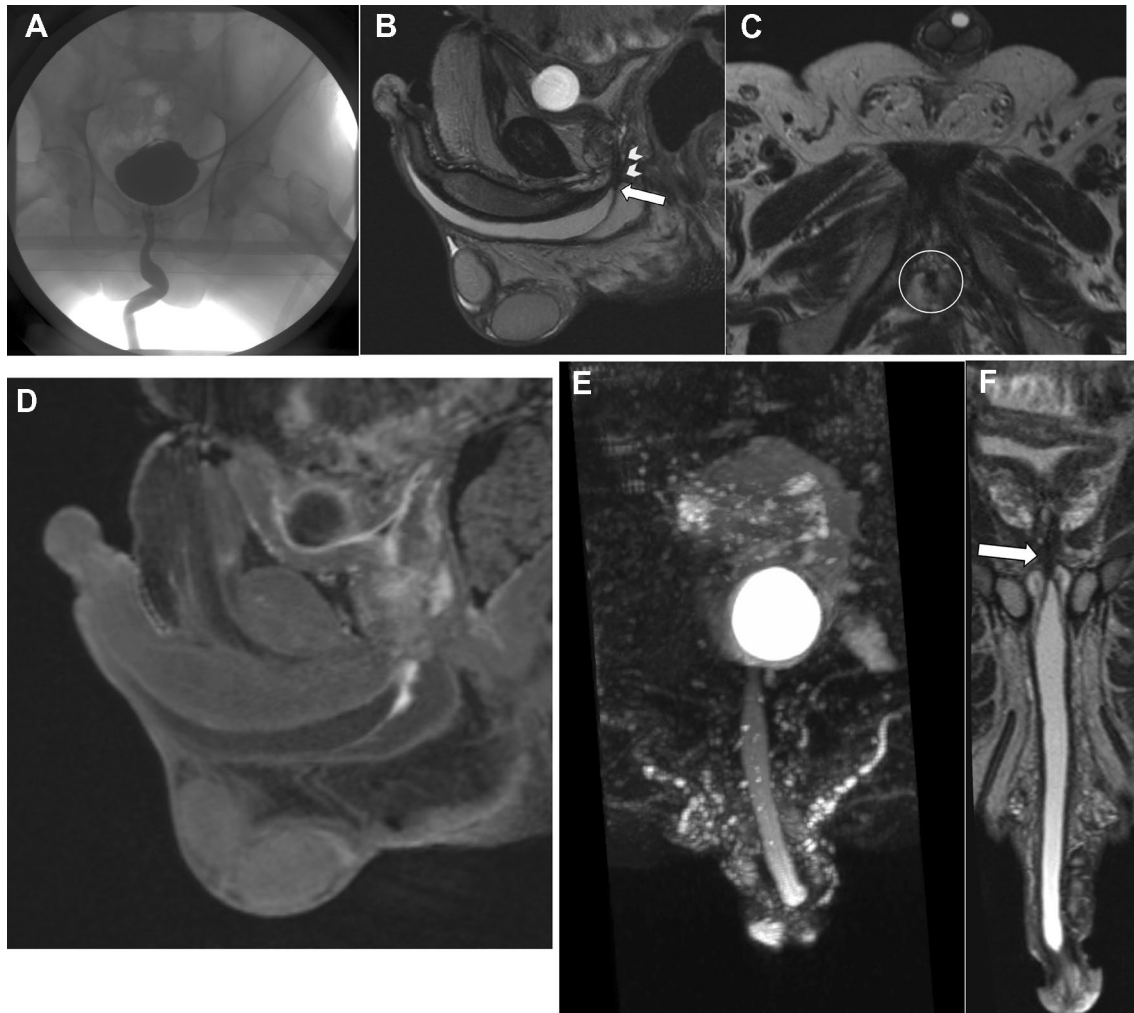


Fig. 14 60-year-old male with a history of complete urinary retention status post suprapubic tube placement and holmium laser enucleation of the prostate, now with inability to void one week postoperatively. **a** Intraoperative RUG combined with cystogram showed inability to push contrast past bladder neck. Stenosis likely in membranous urethra. **b** 3D T2 sagittal shows urethra distended with gel to level of stenosis. The stricture/stenosis (arrow) measures 1.2 cm and involves the proximal bulbar urethra and entire membranous urethra. Associated hypointense fat stranding (arrowheads) concerning for fibrotic change

or scar tissue. **c** 3D T2 axial of prostatic urethra shows irregularity of prostatic urethra (circle) consistent with post treatment changes. **d** T1 sagittal post-contrast images showed delayed contrast enhancement in the membranous and proximal bulbar portions of the urethra, in keeping with spongiofibrosis. **e** MIP reconstruction from 3D T2 FS creates a close approximation of the original RUG image. **f** Curved reconstruction of 3D T2 clearly visualizes length of stenosis (arrow) and relationship to surrounding soft tissues

in evaluating surrounding soft tissues, and the accuracy of its measurements can be compromised when technical factors such as patient positioning are suboptimal. If a skilled operator is available, SUG offers both high-resolution characterization of strictures and assessment of periurethral tissues. Its ability to measure anterior strictures is remarkable, matching intraoperative findings with 100% accuracy. However, SUG can be limited by poor visualization of posterior urethral stenosis especially if a skilled operator is unavailable. The urologist or radiologist should also be provided more direction on when ultrasonography with endorectal probe or SUG combined with RUG is equal to MRI and can

save on cost. We reviewed the potential uses and combinations of the available imaging modalities in the evaluation of urethral stricture disease. In the majority of cases, RUG is sufficient to diagnose and decide for or against surgery, but some cases will benefit from SUG or MRU. The case we provided showed a patient who had a complex history of prostate surgery who needed simultaneous evaluation of an obliterative posterior stricture and evaluation of the prostate. Future studies should focus on expanding the precise criteria for each imaging modality so that the practicing clinician may readily utilize the most effective imaging tools in each clinical scenario.

Funding No funding was received to assist with the preparation of this manuscript.

Declarations

Conflict of interest The authors have no financial or non-financial interests to declare.

References

1. Abdeen BM and Badreldin AM (2021) Urethral Strictures. Treasure Island (FL): StatPearls Publishing. <https://www.statpearls.com/ArticleLibrary/viewarticle/30833>. Accessed 2021 Oct 21.
2. Alwaal A, Blaschko S, McAninch J, Breyer B (2014) Epidemiology of urethral strictures. *Transl Androl Urol* 3(2):209–213. <https://doi.org/10.3978/j.issn.2223-4683.2014.04.07>
3. Verla W, Oosterlinch W, Anne-Françoise S, Waterlooos M (2019) A comprehensive review emphasizing anatomy, etiology, diagnosis, and treatment of male urethral stricture disease. *BioMed Res Int* 9046430. <https://doi.org/10.1155/2019/9046430>
4. Wessells H, Angermeier KW, Elliott S et al (2017) Male urethral stricture: American Urological Association guideline. *J Urol* 2017 197(1):182–190. <https://doi.org/10.1016/j.juro.2016.07.087>
5. EAU Guidelines. Edn. presented at the EAU Annual Congress Milan 2021. ISBN 978-94-92671-13-4.
6. Lumen N, Hoebeke P, Willemsen P, De Troyer B, Pieters R, Oosterlinch W (2009) Etiology of urethral stricture disease in the 21st century. *J Urol* 182(3):983–7. <https://doi.org/10.1016/j.juro.2009.05.023>
7. Jun MS and Santucci RA (2019) Urethral stricture after phalloplasty. *Transl Androl Urol* 8(3):266–272. <https://doi.org/10.21037/tau.2019.05.08>
8. Mundy A and Andrich D (2011) Urethral strictures. *BJU Int* 107(1):6–26. <https://doi.org/10.1111/j.1464-410X.2010.09800.x>
9. Horiguchi A et al. (2020) Magnetic resonance imaging findings of traumatic bulbar urethral stricture help estimate repair complexity. *Urol* 135:146–153. <https://doi.org/10.1016/j.urology.2019.09.036>
10. Heston AL, Esmonde NO, Dugi DD, Berli JU (2019) Phalloplasty: techniques and outcomes. *Transl Androl Urol*. 8(3):254–265. <https://doi.org/10.21037/tau.2019.05.05>.
11. Elliot SP et al. (2022) One-Year Results for the ROBUST III Randomized Controlled Trial Evaluating the Optilume® Drug-Coated Balloon for Anterior Urethral Strictures. *J Urol* 207(4):866–875. <https://doi.org/https://doi.org/10.1097/JU.0000000000002346>
12. Cunningham JH (1910) The diagnosis of stricture of the urethra by Roentgen rays. *Trans Am Assoc Genitourin Surg* 3(5):369–71.
13. Maciejewski C and Rourke K (2015) Imaging of Urethral Stricture Disease. *Transl Androl Urol*. 4(1):2–9. <https://doi.org/10.3978/j.issn.2223-4683.2015.02.03>
14. Bach P and Rourke K (2014). Independently Interpreted Retrograde Urethrography Does Not Accurately Diagnose and Stage Anterior Urethral Stricture: The Importance of Urologist-performed Urethrography. *J Reconstr Urol* 83(5):1190–1194. <https://doi.org/10.1016/j.urology.2013.12.063>
15. Yu NC, Raman S, Patel M, Barbaric Z (2004) Fistulas of the Genitourinary Tract: A Radiologic Review. *Radiographics* 24(5):1331–1352. <https://doi.org/10.1148/rg.245035219>.
16. Osman Y, El-Ghar M, Mansour O, Refaie H, El-Diasty T (2006) Magnetic resonance urethrography in comparison to retrograde urethrography in diagnosis of male urethral strictures: is it clinically relevant? *Eur Urol*. 50(3):587–93. <https://doi.org/10.1016/j.eururo.2006.01.015>
17. Kawashima A et al. Imaging of Urethral Disease: A Pictorial Review (2004). *Radiographics*. 24:S195–S216. <https://doi.org/10.1148/rg.24si045504>
18. Breyer BN, Cooperberg MR, McAninch JW, Master VA (2009) Improper retrograde urethrogram technique leads to incorrect diagnosis. *J Urol* 182:716–17. <https://doi.org/10.1016/j.juro.2009.04.060>
19. Akpayak IC, Ani CC, Dakum NK, Ramyil VM, Shuaibu SI (2012) Sonourethrography in the evaluation of anterior urethral strictures. *J West Afr Coll Surg* 2(1):1–13. PMC4170287.
20. Tao W et al (2019) MR urethrography versus X-ray urethrography compared with operative findings for evaluation of urethral strictures. *Int Urol Nephrol* 51(7):1137–43. <https://doi.org/10.1007/s11255-019-02162-w>
21. Krukowski J, Frankiewicz M, Kałużny A, Matuszewski M (2020) Ultrasonographic assessment of male anterior urethra. Description of the technique of examination and presentation of major pathologies. *Med Ultrason* 22(2):236–242. <https://doi.org/10.11152/mu-2426>
22. Chiou RK, Anderson JC, Tran T, Patterson RH, Wobig R, Taylor RJ (1996) Evaluation of urethral strictures and associated abnormalities using high-resolution and color Doppler ultrasound. *Urol* 47:102–7. [https://doi.org/10.1016/s0090-4295\(99\)80391-4](https://doi.org/10.1016/s0090-4295(99)80391-4)
23. Klosterman PW, Laing FC, McAninch JW (1989) Sonourethrography in the evaluation of urethral stricture disease. *Urol Clin North Am* 16:791–7. PMID: 2683307.
24. Wu AK and McAninch JW (2012) Impact of urethral ultrasonography on decision-making in anterior urethroplasty. *BJU Int* 109:438–42. <https://doi.org/10.1111/j.1464-410X.2011.10246.x>
25. Das S (1992) Ultrasonographic evaluation of urethral stricture disease. *Urol* 40:237–42. [https://doi.org/10.1016/0090-4295\(92\)90481-b](https://doi.org/10.1016/0090-4295(92)90481-b)
26. Arda K, Basar M, Deniz E, Yildiz S, Akpınar L, Olçer T (1995) Sonourethrography in anterior urethral stricture: comparison to radiographic urethrography. *Arch Ital Urol Androl* 67:249–54.
27. Choudhary S, Singh P, Sundar E, Kumar S, Sahai A (2004) A comparison of sonourethrography and retrograde urethrography in evaluation of anterior urethral strictures. *Clin Radiol* 59:736–42. <https://doi.org/10.1016/j.crad.2004.01.014>
28. Gupta N, Dubey D, Mandhani A, Srivastava A, Kapoor R, Kumar A (2006) Urethral stricture assessment: a prospective study evaluating urethral ultrasonography and conventional radiological studies. *BJU Int* 98:149–53. <https://doi.org/10.1111/j.1464-410X.2006.06234.x>
29. Morey AF and McAninch JW (1996) Ultrasound evaluation of the male urethra for assessment of urethral stricture. *J Clin Ultrasound* 24:473–9. [https://doi.org/10.1002/\(SICI\)1097-0096\(199610\)24:8<473::AID-JCU7>3.0.CO;2-H](https://doi.org/10.1002/(SICI)1097-0096(199610)24:8<473::AID-JCU7>3.0.CO;2-H)
30. Gallentine ML and Morey AF (2002) Imaging of the male urethra for stricture disease. *Urol Clin North Am* 29:361–72. [https://doi.org/10.1016/s0094-0143\(02\)00028-9](https://doi.org/10.1016/s0094-0143(02)00028-9)
31. Morey AF and McAninch JW (2000) Sonographic staging of anterior urethral strictures. *J Urol* 163:1070–5. [https://doi.org/https://doi.org/10.1016/S0022-5347\(05\)67696-3](https://doi.org/https://doi.org/10.1016/S0022-5347(05)67696-3)
32. Talreja SM, Tomar V, Yadav SS, Japial U, Priyadarshi S, Agarwal N, Vyas N (2016) Comparison of sonoelastography with sonourethrography and retrograde urethrography in the evaluation of male anterior urethral strictures. *Turk. J Urol*. 42(2):84–91. <https://doi.org/10.5152/tud.2016.99223>
33. Talreja SM, Yadav SS, Tomar V, Agarwal N, Japial U, Priyadarshi S (2016) ‘Real-time sonoelastography’ in anterior urethral strictures: A novel technique for assessment of spongiositis. *Cent. European J Urol*. 69(4):417–424. <https://doi.org/10.5173/ceju.2016.808>
34. Toms AP, Bullock KN, Berman LH (2003) Descending urethral ultrasound of the native and reconstructed urethra in patients with

- hypospadias. *Br J Radiol* 76:260–3. <https://doi.org/10.1259/bjr/98474499>
35. Shahsavari R, Bagheri SM, Iraj H (2017) Comparison of Diagnostic Value of Sonourethrography with Retrograde Urethrography in Diagnosis of Anterior Urethral Stricture. *Open Access Maced J Med Sci*. 5(3):335–339. <https://doi.org/10.3889/oamjms.2017.073>
 36. Frankiewicz M, Markiet K, Krukowski J, Szurowska E, Matuszewski M (2021) MRI in patients with urethral stricture: a systematic review. *Diagn Interv Radiol*. 27:134–146. <https://doi.org/10.5152/dir.2020.19515>
 37. Buckley JC, Wu AK, McAninch JW (2011) Impact of urethral ultrasonography on decision-making in anterior urethroplasty. *BJU International* 109:438–42. <https://doi.org/10.1111/j.1464-410X.2011.10246.x>
 38. El-Ghar M, Osman Y, Elbaz E, Refiae H, El-Diasty T (2010) MR urethrogram versus combined retrograde urethrogram and sonourethrography in diagnosis of urethral stricture. *Eur J Radiol*. 74(3):e193–8. <https://doi.org/10.1016/j.ejrad.2009.06.008>
 39. Hamada T, Takimoto Y, Ono M, Endou M, Henmi K (1992) Observation of the posterior urethra by transrectal linear ultrasonography. *Acta Urol. Jpn*. 38(12):1373–1377. PMID: 1283806.
 40. Wyczółkowski M, Praisner A, Piasecki Z, Pawlicki B (2000) Functional evaluation of the prostatic urethra by means of transrectal ultrasound. *Wiad Lek*. 53(5-6):299–306. PMID: 10983385
 41. Lumen N et al (2021) Urethral Strictures. *European Association of Urology*. <https://uroweb.org/guideline/urethral-strictures/#5>. Accessed 2021 Dec 20.
 42. Dixon C, Hricak H, McAninch J (1992) Magnetic resonance imaging of traumatic posterior urethral defects and pelvic crush injuries. *J Urol*. 148(4):1162–5. [https://doi.org/10.1016/s0022-5347\(17\)36849-0](https://doi.org/10.1016/s0022-5347(17)36849-0)
 43. Sung D et al (2006) Obliterative urethral stricture: MR urethrography versus conventional retrograde urethrography with voiding cystourethrography. *Radiol* 240(3):842–8. <https://doi.org/10.1148/radiol.2403050590>
 44. Oh MM et al (2010) Magnetic resonance urethrography to assess obliterative posterior urethral stricture: comparison to conventional retrograde urethrography with voiding cystourethrography. *J Urol* 183(2):603–7. <https://doi.org/10.1016/j.juro.2009.10.016>
 45. Horiguchi A et al (2022) Role of Magnetic Resonance Imaging in the Management of Male Pelvic Fracture Urethral injury. *Int J Urol* <https://doi.org/10.1111/iju.14779>
 46. Joshi P, Desai D, Shah D, Joshi D, Kulkarni S (2021) Magnetic resonance imaging procedure for pelvic fracture urethral injuries and recto urethral fistulas: A simplified protocol. *Turk J Urol* 47(1):35–42. <https://doi.org/10.5152/tud.2020.20472>
 47. Achenbach S, Moshage W, Ropers D, Bachmann K (1998) Curved Multiplanar Reconstructions for the Evaluation of Contrast-Enhanced Electron Beam CT of the Coronary Arteries. *AJR Amer J Roentgenol*. 170:895–899. <https://doi.org/10.2214/ajr.170.4.9530029>
 48. New Choice Health. <https://www.newchoicehealth.com>. Accessed 2021 December 20.
 49. Aho T, Finch W, Jefferson P, Suraparaju L, Georgiades F (2021) HoLEP for acute and non-neurogenic chronic urinary retention: how effective is it? *World J. Urol* 39(7):2355–2361. <https://doi.org/10.1007/s00345-021-03657-x>
 50. Elsaqa M, Serag M, Leenlani N, et al. (2022) The incidence of urethral stricture and bladder neck contracture with transurethral resection vs. holmium laser enucleation of prostates: A matched, dual-center study. *Can Urol Assoc J*; Epub ahead of print. <http://dx.doi.org/https://doi.org/10.5489/cuaj.7967>
 51. Rosenbaum CM, Vetterlein MW, Fisch M, Reiss P, Worst TS, Kranz J, Steffens J, Kluth LA, Pfalzgraf D (2021) Contemporary Outcomes after Transurethral Procedures for Bladder Neck Contracture Following Endoscopic Treatment of Benign Prostatic Hyperplasia. *J Clin Med*. 10(13):2884. <https://doi.org/10.3390/jcm10132884>

Publisher's Note Springer Nature remains neutral with regard to jurisdictional claims in published maps and institutional affiliations.

Springer Nature or its licensor (e.g. a society or other partner) holds exclusive rights to this article under a publishing agreement with the author(s) or other rightsholder(s); author self-archiving of the accepted manuscript version of this article is solely governed by the terms of such publishing agreement and applicable law.

Authors and Affiliations

Daniel Harris^{1,3}  · Christopher Zhou^{1,3} · Jeffrey Girardot¹ · Ariel Kidron² · Shubham Gupta^{1,2,3} · Andre Guilherme Cavalcanti^{3,4} · Leonardo Kayat Bittencourt^{1,5}

✉ Daniel Harris
dph52@case.edu

¹ Case Western Reserve University School of Medicine, Cleveland, OH, USA

² Nova Southeastern University College of Osteopathic Medicine, Fort Lauderdale, FL, USA

³ Urology Institute, University Hospitals Cleveland Medical Center, Cleveland, OH, USA

⁴ Department of General and Specialized Surgery, Federal University of the State of Rio de Janeiro, Rio de Janeiro, Brazil

⁵ Department of Radiology, University Hospitals Cleveland Medical Center, Cleveland, OH, USA